WJAETS

World Journal of Advanced Engineering Technology and Sciences

eISSN: 2582-8266

Cross Ref DOI: 10.30574/wjaets

Journal homepage: https://wjaets.com/

(Research Article)

ON THE VARIANCE OF THE HISTOGRAM TEST OF ADCS

F. Corrêa Alegria *

Instituto de Telecomunicações and Department of Electrical and Computer Engineering, Instituto Superior Técnico, Technical University of Lisbon, Portugal.
* Corresponding Author

ORCID Details
F. Corrêa Alegria: https://orcid.org/0000-0003-0854-489X

World Journal of Advanced Engineering Technology and Sciences, 2026, 20(02), 175–183

Publication history: Received on 01 July 2026; revised on 17 August 2026; accepted on 19 August 2026

Article DOI: https://doi.org/10.30574/wjaets.2026.20.2.0406

ABSTRACT

The histogram test is one of the most widely used methods for the characterization of analog-to-digital converters (ADCs), yielding estimates of the transition voltages and, from them, of the code bin widths, gain, offset and linearity errors. Since these estimates are computed from a finite number of samples that are affected by several non-idealities of the test setup, they behave as random variables whose uncertainty must be quantified in order to establish a confidence interval for the converter characteristics. This paper presents an overview of that uncertainty, with particular emphasis on the variance of the transition voltages obtained with the cumulative histogram.

The combined influence of the three dominant random effects — phase noise, input-equivalent additive noise and the random phase difference between the stimulus signal and the sampling clock — on the number of counts of the cumulative histogram is analysed within a unified framework, instead of treating each effect separately and adding the individual contributions as was done in earlier works. The variance of the number of counts is decomposed into the mean of the conditional variance and the variance of the conditional mean, and the dependence of each term on the standard deviations of the noise sources and on the transition voltage is examined. Building on this analysis, an asymptotically approximate but more accurate expression for the variance of the transition voltages is presented, whose maximum relative error is below 17%. It reproduces the saturation of the variance towards $M/4$ for large noise by means of a minimum function and accounts for the random phase difference through a maximum function, thereby avoiding the overestimation inherent in the expressions adopted in the de facto standard for ADC testing.

The effect of frequency errors, which cause the sample phases to depart from a uniform distribution, is also addressed, including the coherent-sampling condition, the role of the frequency ratio and of the Farey sequence, and the bound on the frequency error below which the variance of the number of counts remains lower than ¼. Theoretical predictions are validated both against results previously reported in the literature and against experimental measurements performed on real ADCs, showing good agreement in all cases.

Keywords: Analog-to-digital converter; ADC testing; Histogram test; Cumulative histogram; Transition voltages; Measurement uncertainty; Variance; Phase noise; Frequency errors.

1 INTRODUCTION

The histogram test [1][2][3] is one of the most established techniques for characterizing analog-to-digital converters (ADCs). By reconstructing the converter transfer function, it reveals the deterministic properties of the device, from which the gain, the offset, the transition voltages and the code bin widths are readily obtained.

The converter is driven by a stimulus signal whose amplitude density function is known in advance. A sinusoid is the usual choice, since it is the waveform that can most easily be generated with low distortion. A large number of samples is then collected, and the transfer characteristic is recovered by comparing the output codes actually produced with those that an ideal converter would have delivered.

The characterization results are inevitably degraded by the many non-idealities of the test setup — among them the amplitude, offset, frequency, additive noise and phase noise of the stimulus signal, together with the frequency and phase noise of the sampling clock. The additive noise and the aperture uncertainty of the ADC itself, although not quantified by this test method, further corrupt the outcome.

These error sources fall into two broad categories. Deterministic errors bias the results and, once identified, can be compensated; random errors, by contrast, introduce an uncertainty that cannot be removed but that should at least be specified.

Each result can therefore be regarded as a random variable whose distribution may be taken as normal. Once its mean and variance are known, a confidence interval can be built that brackets the true value of the corresponding ADC characteristic with a prescribed level of confidence.

The remainder of the paper is devoted to determining the variance of the transition voltages.

Note that the uncertainty of estimation of the ADC parameters, unavoidable in any estimation procedure, will also affect the results of measurement chains where they are used, whatever the quantity being estimated like magnetic field from eddy currents in non-destructive testing [17] or velocity in a fluid [18], for example.

2 TRANSITION VOLTAGES DETERMINATION

The transition voltages can be estimated in two ways, either from the histogram or from the cumulative histogram. The histogram is obtained by counting how many samples fall in each output code, whereas the cumulative histogram counts, for every code, the samples whose output code is that value or lower. In principle the two routes give the same estimates, but the histogram requires an iterative computation in which errors accumulate. For this reason the cumulative histogram is the one traditionally adopted.

The probability distribution of the transition voltages can thus be recovered from that of the number of counts of the cumulative histogram.

The error sources listed in the previous section are conventionally grouped into three effects:

- *Phase noise*, which lumps together the phase noise of the function generator, the phase noise of the clock generator and the aperture uncertainty of the ADC;
- *Input-equivalent noise*, which gathers the noise of the stimulus signal generator and the additive noise of the ADC[4];
- *Random phase difference*, which arises because the samples are taken at a fixed rate while the instant at which acquisition begins bears no relation to the stimulus signal, so that the signal values at the sampling instants differ from one realization of the test to another. This randomness spreads the sample phases uniformly over one period, which is precisely what allows the expected output codes to be inferred from the amplitude distribution of the stimulus signal. Any error in the stimulus or sampling frequencies destroys this uniform distribution of the sample phases.

3 VARIANCE

The uncertainty in the estimation of the code bin width was first examined by Doernberg et al. in 1984 [5]. Their analysis considered only input-equivalent noise, and only in the regime where its variance is far larger than the ideal code bin width; under those assumptions the sampled voltage was taken to be uniformly distributed within each code bin.

A major step forward was taken by Blair in 1994 [6], who accounted simultaneously for input-equivalent noise and for the random phase difference between the stimulus signal and the sampling clock. He derived uncertainty expressions for both the code bin width and the transition voltages, and these were subsequently incorporated into the de facto standard for ADC testing [7][8].

Phase noise, which Blair had not considered, was later addressed by Chiorboli et al. in 1999 [9], who extended Blair's expressions so as to include it.

In all of these works the three effects were treated one at a time and their individual contributions simply added together.

A unified treatment was proposed in [10], in which the three effects are studied jointly, giving a sharper picture of how each one contributes to the uncertainty of the transition voltages. It was shown there that the probability density function of the number of counts of the cumulative histogram is fixed by the number of acquired samples (M) together with the probability that a given sample belongs to a class of the cumulative histogram (p_k). The mean was found to be

$$\mu_{c_k} = \frac{M}{2\pi}\int_{-\pi}^{\pi} p_k(\gamma)d\gamma \qquad (1)$$

while the variance was given by

$$\sigma_{c_k}^2 = \mu_{\sigma_{c_k|\varphi}^2} + \sigma_{\mu_{c_k|\varphi}}^2 \qquad (2)$$

$$\mu_{\sigma_{c_k|\varphi}^2} = \frac{M}{2\pi}\int_{-\pi}^{\pi} p_k(\gamma)\cdot[1-p_k(\gamma)]\cdot d\gamma \qquad (3)$$

$$\sigma_{\mu_{c_k|\varphi}}^2 = \frac{M}{2\pi}\int_{0}^{2\pi}\left[\sum_{j=0}^{M-1} p_k\left(j\frac{2\pi}{M}+\varphi\right)\right]^2 d\varphi - \left[\frac{M}{2\pi}\int_{-\pi}^{\pi} p_k(\gamma)d\gamma\right]^2 \qquad (4)$$

This probability depends in turn on the normalized standard deviation of the input-equivalent noise (σ_n), defined as the standard deviation of that noise (σ) divided by the stimulus signal amplitude (A); on the standard deviation of the phase noise (σ_θ); and on the normalized transition voltage ($U[k]$) and the sample phase (γ):

$$p_k(\gamma) = \int_{-\infty}^{U[k+1]}\int_{-1}^{1}\frac{\sum_{n=-\infty}^{\infty}\left(e^{\frac{-acos(-y)+\gamma-2\pi n}{2\sigma_\theta^2}} + e^{\frac{acos(-y)+\gamma-2\pi n}{2\sigma_\theta^2}}\right)}{2\pi\sigma_n\sigma_\theta\sqrt{1-y^2}} e^{\frac{-(u-y)^2}{2\sigma_n^2}} dydu \qquad (5)$$

The variance was split into two contributions, referred to as the “mean of the conditional variance” ($\mu_{\sigma_{c_k|\varphi}^2}$) and the “variance of the conditional mean” ($\sigma_{\mu_{c_k|\varphi}}^2$).

3.1 Mean of the conditional variance

The way $\mu_{\sigma_{c_k|\varphi}^2}$ depends on the standard deviations of the phase noise and of the input-equivalent noise, established in [10], is shown in Fig. 1.

As equation (3) makes clear, this term is directly proportional to the number of samples (M). For small standard deviations it grows linearly with them and, when only one of the two noise sources is present, the rate of growth is the same in either case.

$$\mu_{\sigma_{c_k|\varphi}^2}\big|_{\sigma_\theta=0} \longrightarrow_{\sigma_n\to 0} \frac{M}{\pi\sqrt{\pi}}\sigma_n$$

$$\mu_{\sigma_{c_k|\varphi}^2}\big|_{\sigma_n=0} \longrightarrow_{\sigma_\theta\to 0} \frac{M}{\pi\sqrt{\pi}}\sigma_\theta \qquad (6)$$

The same rate was reported in [6] for input-equivalent noise acting alone ($\frac{1.13M}{2}$). At large standard deviations, however, $\mu_{\sigma_{c_k|\varphi}^2}$ saturates towards $\frac{M}{4}$ — a behaviour that [6] overlooked for the cumulative histogram, and hence for the transition voltages, where the dependence on the standard deviation was assumed to remain linear throughout. The same simplification was made in [9] for phase noise alone.

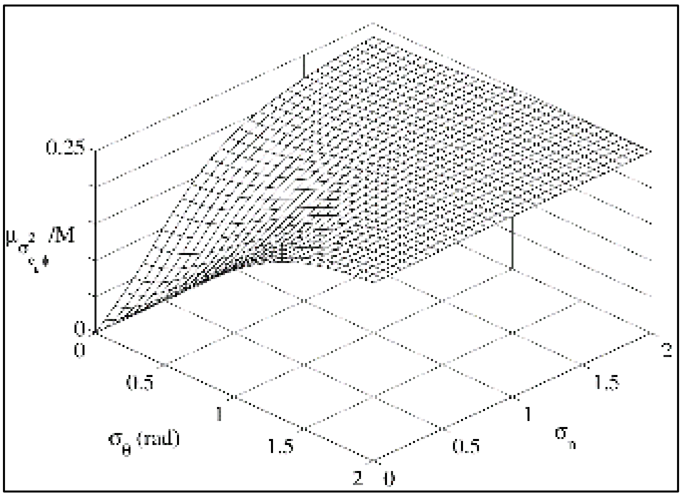

Figure 1: The term $\mu_{\sigma^2_{c_k|\varphi}}$, normalized to the number of acquired samples (*M*), for a transition voltage equal to the stimulus signal offset (*U*[*k*+1]=0), plotted against the standard deviation of the phase noise (σ_θ) and the standard deviation of the input-equivalent noise normalized to the stimulus signal amplitude (σ_n).

3.2 Variance of the conditional mean

The dependence of $\sigma^2_{\mu_{c_k|\varphi}}$ on the number of samples and on the transition voltage is more intricate than that of $\mu_{\sigma^2_{c_k|\varphi}}$. Fig. 2 displays this term when phase noise is absent; when instead the input-equivalent noise is absent, its dependence on the standard deviation of the phase noise closely resembles the curve of Fig. 2.

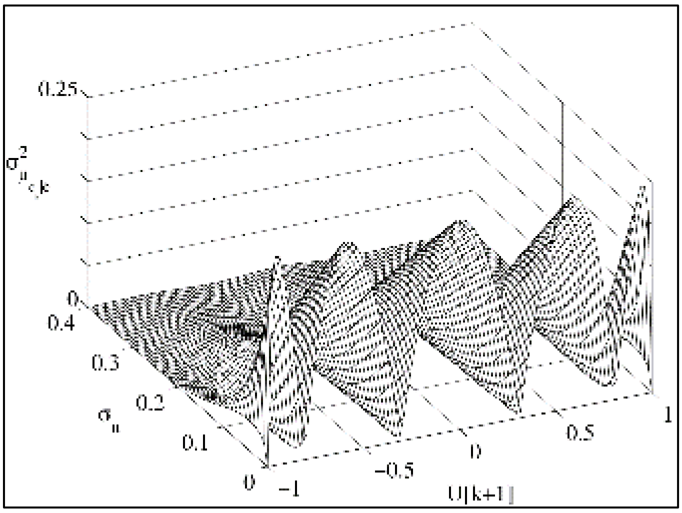

Figure 2: The term $\sigma^2_{\mu_{c_k|\varphi}}$ in the absence of phase noise (σ_θ=0) with 5 acquired samples, plotted against the normalized transition voltage (*U*[*k*+1]).

At small noise standard deviations, $\sigma^2_{\mu_{c_k|\varphi}}$ varies strongly with the transition voltage, and the number of arcs visible in Fig. 2 equals the number of samples.

Its largest value, ¼, is reached when phase noise is absent. In the presence of an error in the stimulus or sampling frequency this value may be exceeded, as reported in [13].

As the noise standard deviation grows, $\sigma^2_{\mu_{c_k|\varphi}}$ falls off, tending to zero for large values (Fig. 3).

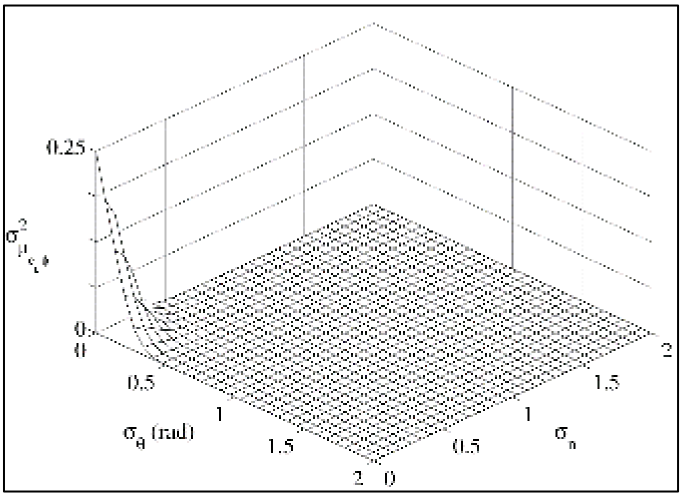

Figure 3: The term $\sigma^2_{\mu_{c_k|\varphi}}$ for a transition voltage equal to the stimulus signal offset ($U[k+1]=0$) with 5 acquired samples, plotted against the standard deviation of the phase noise (σ_θ) and the standard deviation of the input-equivalent noise normalized to the stimulus signal amplitude (σ_n).

For small standard deviations it decreases linearly, at the same rate as $\mu_{\sigma^2_{c_k|\varphi}}$.

In [6] the random phase difference between the sampling clock and the stimulus signal was handled independently of the input-equivalent noise, which amounts to assuming its contribution to be the same at every value of the standard deviation.

3.3 Variance of the number of counts

Adding the two terms $\mu_{\sigma^2_{c_k|\varphi}}$ and $\sigma^2_{\mu_{c_k|\varphi}}$ yields the variance of the number of counts, which is plotted in Fig. 4.

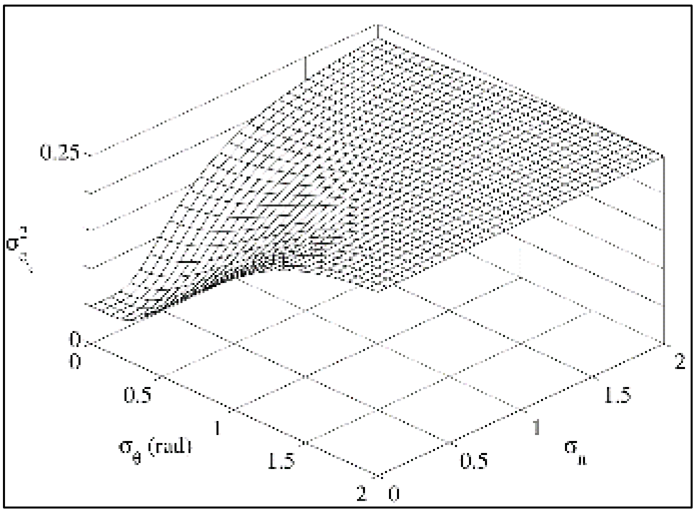

Figure 4: The term $\sigma^2_{c_k}$ for a transition voltage equal to the stimulus signal offset ($U[k+1]=0$) with 5 acquired samples, plotted against the standard deviation of the phase noise (σ_θ) and the standard deviation of the input-equivalent noise normalized to the stimulus signal amplitude (σ_n).

At large standard deviations this variance tends to $\frac{M}{4}$, just as $\mu_{\sigma^2_{c_k|\varphi}}$ does, whereas at small standard deviations it flattens out at the constant value ¼.

3.4 Variance of the transition voltages

An asymptotically approximate expression for the variance of the transition voltages was put forward in [10]: $\sigma^2_T \simeq$

$$\left(\frac{A\pi}{M}\right)^2 max\left(\frac{1}{4}, Mmin\left(\frac{1}{4}, \frac{\sqrt{\left(\frac{\sigma}{A}\right)^2+\sigma_\theta^2}}{\pi\sqrt{\pi}}\right)\right) \quad (7)$$

The maximum relative error incurred by equation (7) stays below 17%. It should be stressed that this figure refers to the error interval of the transition voltages obtained with the histogram method, not to the transition voltages themselves. No closed-form exact expression exists, although more accurate — and correspondingly more involved — ones could be derived.

For comparison, the expression given in [6] is reproduced below in the notation of the present paper:

$$\sigma_T^2 \simeq \left(\frac{A\pi}{M}\right)^2\left(\frac{M}{\pi\sqrt{\pi}}\frac{\sigma}{A} + \frac{1}{\sqrt{\pi}}\frac{M}{\pi}\sigma_\theta + \frac{1}{4}\right) \quad (8)$$

This form is less accurate than the one proposed here: its variance diverges as the standard deviation grows without bound, instead of levelling off at $\frac{M}{4}$. That saturation is exactly what the minimum function in equation (7) reproduces.

In the conventional histogram test, driven by a full-scale stimulus, the input-equivalent noise is usually far smaller than the signal amplitude ($\sigma_n \ll 1$). There is, however, a variant based on small-amplitude stimulus signals [11], [12] in which the two may become comparable.

The random phase difference between the stimulus signal and the sampling clock is better described by the maximum function in equation (7) than by adding a separate contribution (the term ¼ in equation (8)), as was done in [6] at the cost of overestimating the variance.

4 FREQUENCY ERRORS

So that every code has the same chance of being exercised, the samples must span an integer number D of periods of the input signal. If M denotes the number of samples acquired, the stimulus frequency (f) and the sampling frequency (f_s) have to obey the relation

$$\rho = \frac{f}{f_s} = \frac{D}{M} \quad (9)$$

This condition alone does not make the sample phases evenly spaced; for that, D and M must in addition be mutually prime [9], [10].

In practice these frequencies are never met exactly, so the sample phases depart from the intended uniform spacing. The impact of errors in both frequencies on the variance of the cumulative histogram was analysed in [13].

Fig. 5 shows a three-dimensional plot of σ_c^2 for the noise-free case.

The variable α is the length of the phase interval over which the samples belong to a given class of the cumulative histogram, and it is directly tied to the normalized transition voltage $U[k]$ (the transition voltage divided by the stimulus signal amplitude). Fig. 5 shows that when ρ is a rational number whose denominator is 5 (M) and whose numerator is mutually prime with 5, the peak value of the variance over α reaches a minimum (ρ: 0.2; 0.4; 0.6 and 0.8). Conversely, when ρ belongs to the Farey sequence [14] of order 4 (M−1), the variance shows a local maximum (ρ: 0.25; 0.33; 0.5; 0.66 and 0.75). The Farey sequence of order P consists of the rational numbers, listed in increasing order, whose denominator does not exceed P.

When frequency errors are present, it is this value of the variance — the one plotted in Fig. 5 — that should replace the leading term ¼ in equation (7). That ¼, which also appears in (7), is simply the maximum of the variance over α when no frequency error is present.

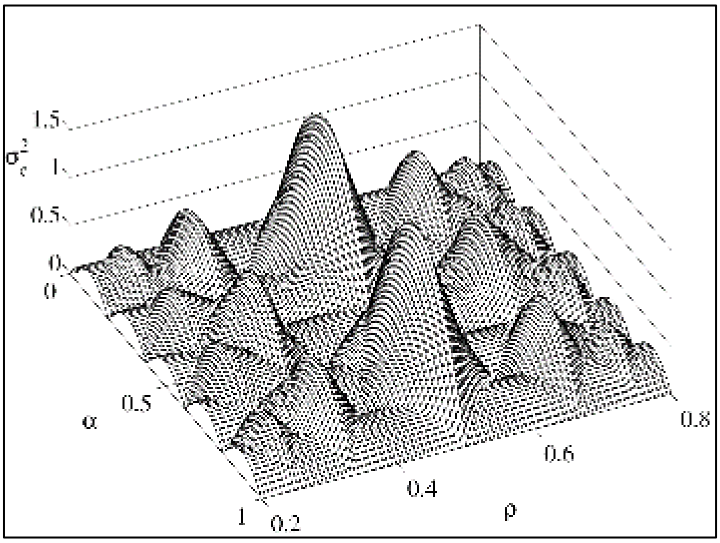

Figure 5: σ_c^2 for different values of α and ρ.

Fig. 6 plots the variance of the number of counts against the phase interval length for M=7. In the absence of frequency error (dashed line) the curve consists, as expected, of seven identical parabolic arcs whose maximum is ¼. Even when a frequency error is present, the variance stays at or below ¼ provided that

$$\frac{\Delta\rho}{\rho} \leq \frac{1}{2DM} \qquad (10)$$

as demonstrated in [13]; this situation is shown by the solid line in Fig. 6.

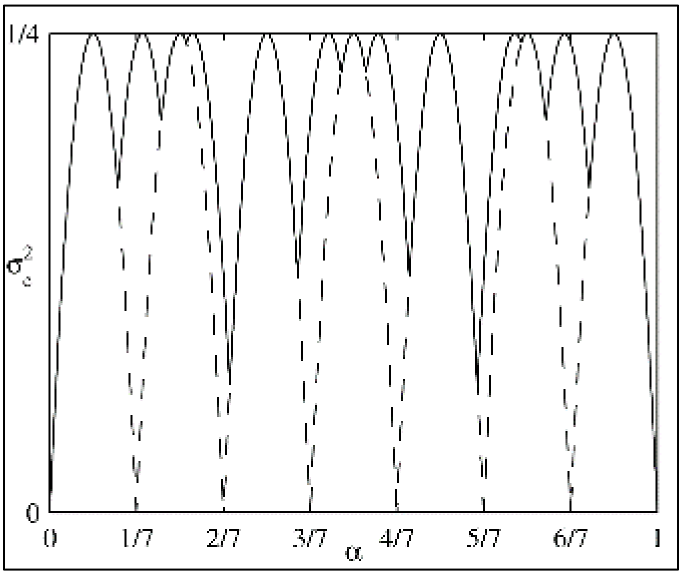

Figure 6: σ_c^2 as a function of α for D=2 and M=7, for ρ=D/M (dashed line) and ρ=D/M+1/2M^2 (solid line).

The curves of Fig. 6 coincide with those of Figure 2 of [15], which confirms the approach followed here.

The work of [10], [16] was also checked against measurements on real ADCs [13], the results of which appear in Fig. 7. In that experiment, 5 samples were taken with a 100 kHz sampling clock while a triangular stimulus of 30 kHz was applied. A frequency error is present here because the ratio of stimulus to sampling frequency (ρ) fails to satisfy (9):

$$\rho = \frac{30{,}000}{100{,}000} = \frac{3}{10} = \frac{1.5}{5} \qquad (11)$$

Fig. 7 shows close agreement between the measured values, drawn as vertical bars that convey the uncertainty in the estimated variances, and the theoretical prediction (solid line).

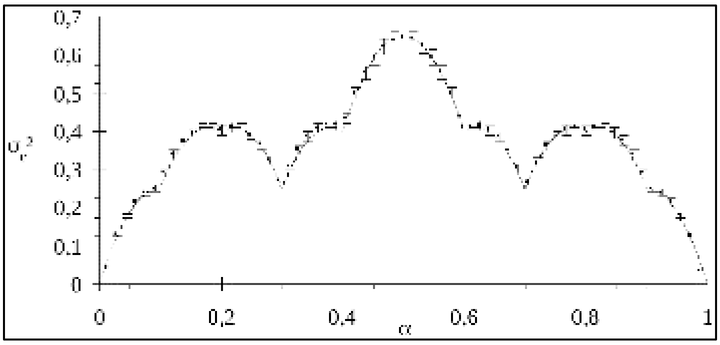

Figure 7: Experimental values of the variance of the number of counts of the cumulative histogram (dots) for a 50% frequency error (M=5). The vertical bars mark the 99.9% confidence interval and the solid line is the theoretical variance.

5 CONCLUSIONS

This paper has reviewed the study of the uncertainty affecting the transition voltages measured with the histogram method, with particular attention to the authors' contributions on the subject [10], [13], [16].

An asymptotically approximate expression for that uncertainty was obtained which is more accurate than the one adopted in the de facto standard [7] and later extended in [9]. It yields a better estimate of the uncertainty of the transition voltages and a tighter sizing of the number of samples required, and hence a shorter test.

No analytical expression for the variance in the presence of frequency errors is yet available; for small errors the value ¼ may be used. Being able to compute the variance of the number of counts for any value of α nonetheless makes it possible to quantify the uncertainty whenever, for whatever reason, an ADC has been tested with frequencies that do not satisfy (9).

The results reported here are currently being considered for inclusion in the IEEE standard for ADC characterization.

Work nevertheless remains to be done, notably the analysis of the uncertainty of the code bin widths and the derivation of an analytical expression for the variance when frequency errors are present.

STATEMENTS ON COMPLIANCE WITH ETHICAL STANDARDS

Disclosure of conflict of interest

The authors declare that there is no conflict of interest.

REFERENCES

[1] F. Corrêa Alegria, A. Cruz Serra, "Error in the estimation of transition voltages with the standard histogram test of ADCs", Measurement 35 (4), pp. 389-397. https://doi.org/10.1016/j.measurement.2004.03.003.

[2] A. Cruz Serra, F. Corrêa Alegria, R. Martins, M. Fonseca da Silva, "Analog-to-digital converter testing—new proposals", Computer Standards & Interfaces 26 (1), pp. 3-13, 2004. https://doi.org/10.1016/S0920-5489(03)00057-6.

[3] A. Cruz Serra, F. Corrêa Alegria, L. Michaeli, P. Michalko, J. Saliga, "Fast ADC testing by repetitive histogram analysis", 2006 Proc. of the IEEE Instrumentation and Measurement Technology Conference, pp. 1633-1638, 2006. ISBN: 0-7803-9360-0/06/$20.00 ©2006 IEEE.

[4] P. Carbone and D. Petri, "Noise Sensitivity of the ADC Histogram Test", Proceedings of the IEEE Instrumentation and Measurement Technology Conference, St. Paul, Minnesota, May 18–20, 1998, pp. 88–91.

[5] J. Doernberg, H.-S. Lee and D. A. Hodges, "Full-Speed Testing of A/D Converters", IEEE Journal of Solid-State Circuits, vol. SC-19, no. 6, pp. 820–827, December 1984. https://doi.org/10.1109/JSSC.1984.1052232.

[6] J. Blair, "Histogram Measurement of ADC Nonlinearities", IEEE Transactions on Instrumentation and Measurement, vol. 43, no. 3, pp. 373–383, June 1994. https://doi.org/10.1109/19.293454.

[7] IEEE Std 1057-1994, "IEEE Standard for Digitizing Waveform Recorders", The Institute of Electrical and Electronics Engineers, Inc., New York, December 1994.

[8] IEEE standard for terminology and test methods for Analog-to-Digital Converters - IEEE Std 1241-2000, pp. 1-98, June 2001. http:\doi.org\10.1109/IEEESTD.2001.92771.

[9] G. Chiorboli and C. Morandi, "About the Number of Records to be Acquired for Histogram Testing of A/D Converters using Synchronous Sinewave and Clock Generators", Proceedings of the 4th Workshop on ADC Modelling and Testing, Bordeaux, France, September 9–10, 1999, pp. 182–186.

[10] F. Corrêa Alegria and A. Cruz Serra, "Uncertainty in the ADC Transition Voltages Determined with the Histogram Method", Proceedings of the IMEKO 2001 Congress, September 2001, Lisbon, Portugal.

[11] F. Alegria, P. Arpaia, A. Cruz Serra and P. Daponte, "ADC Histogram Test by Triangular Small-Waves", Proceedings of the 18th IEEE Instrumentation and Measurement Technology Conference, May 2001, Budapest, Hungary.

[12] F. Alegria, P. Arpaia, A. Cruz Serra and P. Daponte, "ADC Histogram Test using Small-Amplitude Input Waves", Measurement, vol. 31, no. 4, pp. 271-279, June 2002, Elsevier. https://doi.org/10.1016/S0263-2241(01)00043-4.

[13] F. Corrêa Alegria and A. Cruz Serra, "Influence of Frequency Errors in the Variance of the Cumulative Histogram", IEEE Transactions on Instrumentation and Measurement, vol. 50, no. 2, April 2001, pp. 461-464. https://doi.org/10.1109/19.918166.

[14] R. Graham, D. Knuth and O. Patashnik, Concrete Mathematics, 2nd edition, Addison-Wesley, 1994.

[15] P. Carbone and G. Chiorboli, "ADC Sinewave Histogram Testing with Quasi-coherent Sampling", Proceedings of the 17th IEEE Instrumentation and Measurement Technology Conference, vol. 1, pp. 108–113, May 2000, Baltimore, USA.

[16] F. Corrêa Alegria and A. Cruz Serra, "Variance of the Cumulative Histogram of ADCs due to Frequency Errors", Proceedings of the 18th IEEE Instrumentation and Measurement Technology Conference, May 2001, Budapest, Hungary.

[17] O. Postolache, H.G. Ramos, A.L. Ribeiro, F. Corrêa Alegria, "GMR based eddy current sensing probe for weld zone testing", Proc. IEEE Sensors, Christchurch, New Zealand, Vol. 1, pp. 73-78, 2009. ISBN: 978-1-4244-5335-1/09/$26.00 ©2009 IEEE.

[18] O. Birjukova, S. Guillén Ludeña, F. Corrêa Alegria, A. Heleno Cardoso, "Three dimensional flow field at confluent fixed-bed open channels", Proceedings of River Flow 2014, Vol. 1, pp. 1007-1014, September 2014. https://doi.org/10.1201/b17133-136.